Reproducibility Studies with ^{11}C-DTBZ, a Monoamine Vesicular Transporter Inhibitor in Healthy Human Subjects

Grace L.Y. Chan, James E. Holden, A. Jon Stoessl, Ali Samii, Doris J. Doudet, Teresa Dobko, K. Scott Morrison, Michael Adam, Michael Schulzer, Donald B. Calne and Thomas J. Ruth

TRIUMF and Neurodegenerative Disorders Center, University of British Columbia, Vancouver, British Columbia; and Department of Medical Physics, University of Wisconsin, Madison, Wisconsin

The reproducibility of (±)-α-[^{11}C] dihydrotetrabenazine (DTBZ) measures in PET was studied in 10 healthy human subjects, aged 22–76 y. **Methods:** The scan-to-scan variation of several measures used in PET data analysis was determined, including the radioactivity ratio (target-to-reference), plasma-input Logan total distribution volume (DV), plasma-input Logan B_{max}/K_d and tissue-input Logan B_{max}/K_d values. **Results:** The radioactivity ratios, plasma-input B_{max}/K_d and tissue-input B_{max}/K_d all have higher reliability than plasma-input total DV values. In addition, measures using the occipital cortex as the reference region have higher reliability than the same measures using the cerebellum as the reference region. **Conclusion:** Our results show that DTBZ is a reliable PET tracer that provides reproducible in vivo measurement of striatal vesicular monoamine transporter density. In the selection of reference regions for DTBZ PET data analysis, caution must be exercised in circumstances when DTBZ binding in the occipital cortex or the cerebellum may be altered.

Key Words: [^{11}C]dihydrotetrabenazine; PET imaging; vesicular monoamine transporter 2

J Nucl Med 1999; 40:283–289

Dihydrotetrabenazine (DTBZ) is one of the metabolites of tetrabenazine (TBZ), a high-affinity inhibitor of the type 2 vesicular monoamine transporter (VMAT). Like TBZ, DTBZ binds to the VMAT and blocks the storage of monoamine neurotransmitters in presynaptic vesicles (*1,2*). TBZ and its analogs, methoxytetrabenazine (MTBZ) labeled with either ^{11}C or ^{3}H and DTBZ labeled with ^{3}H, have been used extensively to study the distribution and density of VMAT in the substantia nigra and striatum in autoradiographic animal studies (*2–5*) and in postmortem studies in patients with Parkinson's and Alzheimer's diseases (*6,7*). TBZ and its analogs may be better tracers of the integrity of dopamine terminals than are iodinated or fluorinated tropanes (2β-carbomethoxy-3β-[4-iodophenyl]tropane, 2β-carbomethoxy-3β-(4-fluorophenyl)tropane, analogs or 6-[^{18}F]fluoro-L-dopa due to the lack of regulation of the VMAT system compared to the highly regulated dopamine transporter and decarboxylase enzyme (*8,9*). Accordingly, DTBZ labeled with ^{11}C has recently been used in conjunction with PET to examine in vivo the integrity of striatal presynaptic monoaminergic terminals (*10,11*) and to estimate neuronal losses in normal aging (*12*) and neurodegenerative diseases (*12,13*). Compared to TBZ or MTBZ, DTBZ appears to be a better ligand for in vivo PET studies, due to its limited peripheral metabolism, resulting in only polar metabolites that do not cross the blood-brain barrier. In this study, we repeated DTBZ PET scans in 10 healthy human subjects and examined the scan-to-scan variation in several measures used in PET data analysis, including the radioactivity (target-to-reference) ratio, plasma-input Logan B_{max}/K_d values and tissue-input Logan B_{max}/K_d values. The usefulness of these measures to reflect changes in VMAT density depends on their reproducibility. Since VMAT is present in all brain areas, there is no true nonspecific binding region for DTBZ. However, the frontal cortex has been used as a reference region in DTBZ PET studies (*12,13*) because of findings of low VMAT2 binding in the cortical regions from in vitro rodent and human brain studies and low levels of monoamines in cortical areas of the human brain. The cerebellum also has a low density of monoamine terminals. Thus (±)-α-[^{11}C]DTBZ PET data using the cerebellum and the occipital cortex as reference regions were compared to determine which region is most reliable.

Received Jan. 22, 1998; revision accepted Jun. 4 1998.

For correspondence or reprints contact: Grace Lap-Yu Chan, PhD, Rm. G343, ACU, PET, Vancouver Hospital and Health Sciences Center, UBC Site, 2211 Westbrook Mall, Vancouver, BC, Canada V6T 2B5.

MATERIALS AND METHODS

Chemistry

A modification of the method described by Kilbourn et al. (*14*) was used to synthesize (±)-α-[^{11}C]DTBZ. Briefly, (±)-9-O-desmethyl-α-DTBZ was methylated with ^{11}C-methyliodide in a mixture of dimethyl sulfoxide/sodium hydroxide. The product was purified by high-performance liquid chromotography and obtained with > 95% radiochemical purity. The specific activity was 1501 ± 1008 Ci/mmol (mean ± SD) (range 321–3204 Ci/mmol) at ligand injection.

Subjects

Ten healthy subjects, 4 men and 6 women, aged 22–76 y (mean ± SD, 55 ± 18 y) participated in the study. None had neurological disease by history or by clinical examination. Each subject had two (±)-α-[^{11}C]DTBZ PET scans, with the second scan between 3.0 and 12.6 wk after the first (40.1 ± 19.5 d). All subjects gave written informed consent before each scan. The study was approved by the University of British Columbia Human Ethics Committee.

PET Scans and Blood Sampling

PET scans were performed in two-dimensional mode using an ECAT 953B/31 tomograph (CTI/Siemens, Knoxville, TN). The subject was positioned supine in the gantry and with the head centered in the field of view. A thermo-plastic mask was molded to the subject's head to minimize movement and the same mask was used in repositioning for the second scan. Before injection of (±)-α-[^{11}C]DTBZ, a transmission scan with ^{68}Ge rods was obtained for attenuation correction. (±)-α-[^{11}C]DTBZ (237 ± 36 MBq in 10 mL saline) was injected intravenously over 60 s using a Harvard infusion pump. Arterial blood samples were obtained from the radial artery for measurement of total radioactivity and metabolite analysis. For assessment of total radioactivity, 6 arterial blood samples were collected during the first minute immediately after tracer injection, followed by another 6 samples in the second minute and thereafter at 3, 4, 5, 7, 10, 15, 20, 30, 40, 50 and 60 min. Additional arterial blood samples were collected at 15, 30, 45 and 60 min and analyzed by a solid-phase extraction method (*12*). Briefly, plasma was mixed with an equal volume of phosphate-buffered saline and passed through an ^{18}C Sep-Pak column (Waters Mississauga, Ontario, Canada). The column was then washed with 6 mL of phosphate-buffered saline/ethanol (65:35). The column (containing the unchanged DTBZ) and the washes (containing the metabolites) were counted for ^{11}C radioactivity, and the data were used to determine the percentage of unchanged ligand in plasma at these time points. The PET scan protocol included 4 × 1 min, 3 × 2 min, 8 × 5 min and 1 × 10 min sequential emission scans starting at tracer injection for a total acquisition time of 60 min.

Data Analysis

For each scan, 7 consecutive axial slices containing the striatum (caudate and putamen) were summed to produce a composite image. On this summed image, regions of interest (ROIs) were placed over the left and right striatum as follows: one circular ROI on the caudate nucleus (CAU) (61 mm^2) and three circular ROIs (61 mm^2 each) on the putamen (PUT) (Fig. 1). Three circular ROIs (297 mm^2 each) were placed on the occipital cortex (OC) bilaterally, using the same summed image. These ROIs were then applied to the same summed 7 slices of each of the 16 time frames. Additionally, 2 consecutive slices containing the cerebellum (CE) were summed, and 1 oval ROI (556 mm^2) was placed bilaterally on the cerebellum of the summed image and then applied to the 16 time frames. Decay-corrected time-activity curves for the left and right caudate, putamen, occipital cortex and cerebellar ROIs were obtained. Values of the measures related to the putamen were an average of the three ROIs placed on this structure.

The time-activity curves were averaged over all time frames from 30 to 60 min postinjection. These average values were used to generate values for radioactivity ratios. Ratios of the activity in caudate and putamen to both the occipital cortex (CAU/OC, PUT/OC) and to cerebellum (CAU/CE, PUT/CE) were determined. Total (specific and nonspecific) distribution volumes (DVs) using metabolite-corrected plasma time courses as the reference input function were estimated for caudate (DV_{CAU}), putamen (DV_{PUT}), occipital cortex (DV_{OC}) and cerebellum (DV_{CE}) (*15*). In addition, the binding potential B_{max}/K_d was calculated using the formula: $[(DV_{target}/DV_{reference}) - 1]$, with either the occipital cortex or cerebellum as the reference region (referred to as plasma-input B_{max}/K_d). Furthermore, distribution volume ratios (DVRs), using the radioactivity-time courses in occipital cortex or cerebellum as the reference tissue input function, were determined by the method of Logan et al. (*16*). Values of the kinetic rate constant k_2 required by this approach were evaluated by conventional compartmental fitting of the reference tissue time courses. Since our goal was to evaluate the reliability of this approach performed without blood sampling and metabolite analysis, the population mean values for k_2 (cerebellum, 0.086/min; occipital cortex, 0.073/min) were used in these calculations. Values of the binding potential B_{max}/K_d were then derived from the formula (DVR − 1) (referred to as tissue-input B_{max}/K_d). The use of k_2, rather than the more complex combination of rate constants appropriate to a compound that undergoes specific binding in the reference region, is further justified by the rapid rate of equilibration of all kinetic components with this compound. Because of this rapid approach to equilibrium, the effect of the second, k_2-dependent term in the calculation of the

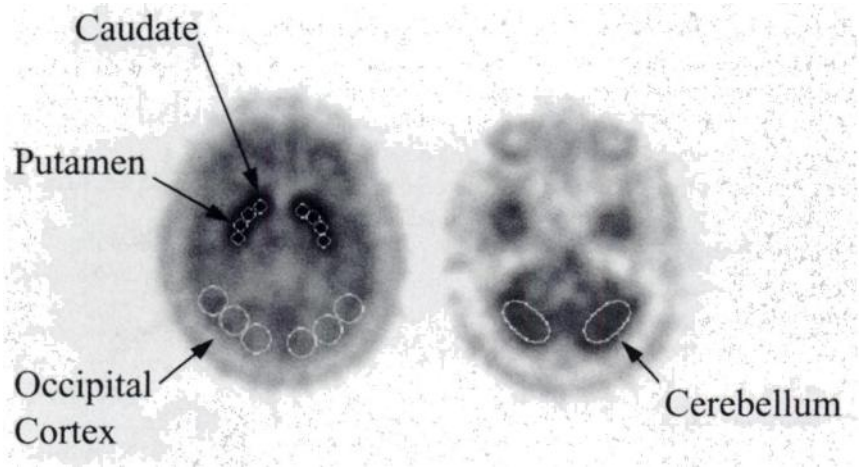

FIGURE 1. Typical placement of ROIs. Left image shows placement of one circular ROI on caudate, three circular ROIs on putamen and three circular ROIs on occipital cortex. Right image shows placement of one oval ROI on cerebellum. ROIs were placed bilaterally.

abscissa values in the Logan graphical analysis is minimal. A trial analysis performed without the second term reduced the total DV values by less than 4%.

Statistical Analysis

Paired *t* tests performed between the left and the right values of the radioactivity ratios, the plasma-input B_{max}/K_d and the tissue-input B_{max}/K_d in both the first and second studies, showed no significant left/right differences. Our data are thus presented as the average of the left and right sides.

A one-way analysis of variance (ANOVA) was performed to obtain the mean, the SD between subjects (SDB) and the SD within subjects (SDW). Confidence intervals for SDW were calculated using chi square distribution. The reliability coefficients (Rs) were estimated from the formula (*17*):

$$R = SDB^2/(SDB^2 + SDW^2).$$

R indicates the reproducibility of the measurements over time, since it measures the intraclass correlation, that is, the correlation between two measurements observed in the same individual at different times.

The reproducibility of all the measures was also assessed by simply calculating the absolute percent change in the values of the measure between the first and the second scan, as follows:

[(value from the second scan

− value from the first scan)/mean value of the 2 scans] × 100%.

For metabolite data, the ratios of metabolite to unchanged DTBZ were plotted versus time, and linear correlation analysis was used to test the line fit and determine the slope. Slopes were also subjected to one-way ANOVA to obtain SDB, SDW and R.

The radioactivity ratios, plasma-input B_{max}/K_d and tissue-input B_{max}/K_d values of caudate or putamen were subjected to linear regression by pairs. The correlation coefficient (r) obtained from the least squares regression line was compared to the critical values at the 5% level of significance. A correction for multiple comparisons in these linear correlations was not performed because it would be too stringent, considering the small number of subjects studied.

RESULTS

After injection of (±)-α-[^{11}C]DTBZ, radioactivity in the arterial plasma peaked rapidly followed by an exponential decline. The radioactivity appeared rapidly in the brain. Figure 2 shows the time-radioactivity curves of several brain regions, as well as the time courses of unchanged ligand in the arterial plasma of a representative subject. The fractions of unchanged DTBZ in plasma were 0.80 ± 0.05 at 15 min, 0.64 ± 0.07 at 30 min, 0.53 ± 0.07 at 45 min and 0.47 ± 0.06 at 60 min after injection. Figure 3 shows representative Logan plots from one of the subjects.

The results of one-way ANOVA on the different measures for DTBZ, with either occipital cortex or cerebellum as the reference region, are shown in Table 1.

The radioactivity ratio, plasma-input B_{max}/K_d and tissue-input B_{max}/K_d have similar reliability. The reliability of the total DV values was low, compared to the other measures. Of all the measures analyzed, the reliability was higher when

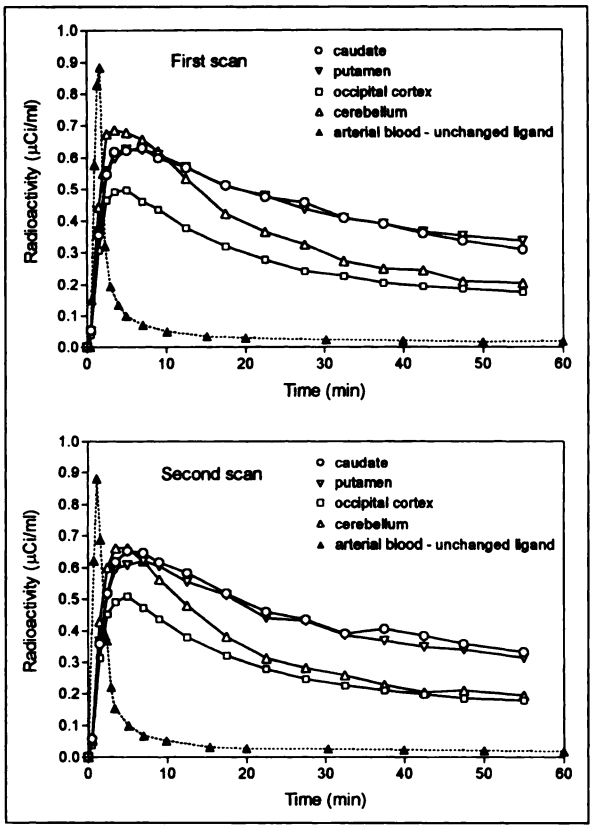

FIGURE 2. Time-radioactivity curves of several brain regions of healthy human subject after receiving intravenous injection of ~7 mCi (±)-α-[^{11}C]DTBZ. Second scan (bottom) was taken 3 wk after first (top). Also shown is time course of unchanged DTBZ in arterial plasma.

the occipital cortex instead of the cerebellum was used as a reference region.

Table 2 shows the absolute percent change in the values of the different measures between the first and second scan, presented as the mean, one SD and the range within the 10 subjects studied. For plasma-input total DV, the average absolute percent change was about 12%, whereas the average absolute percent change of the other measures was about 4% – 6%.

Figure 4 demonstrates the reproducibility of several extracted measures, presented as the values derived from the second scan plotted against those from the first scan. Data for putamen are presented as representative examples. Derived measures include radioactivity ratios, plasma-input B_{max}/K_d and tissue-input B_{max}/K_d values, with the occipital cortex as the reference region. Note that for the different measures, the data points were all very close to the line of identity that represents the perfect agreement line for the values of that measure between the first and second scans.

The slopes obtained from linear regression of the ratio of metabolite to unchanged DTBZ versus time were 0.022 ± 0.005 (mean ± 1 SD) for the first study (r = 0.959–0.998, P = 0.001–0.040) and 0.021 ± 0.006 for the second study (r = 0.964–0.999, P = 0.001–0.121). The SDB, SDW and R for the slopes were 20%, 16% and 60%, respectively.

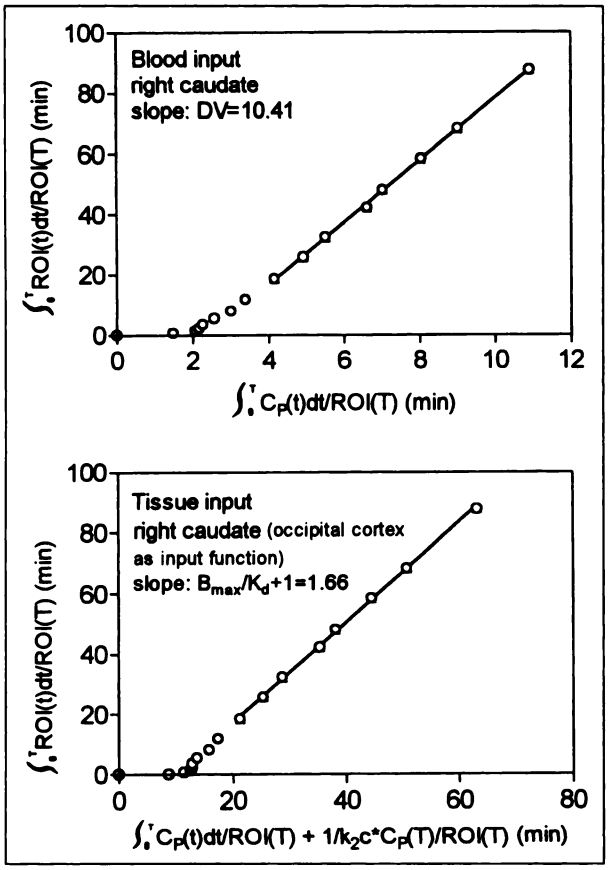

FIGURE 3. Representative Logan plots show estimate of total DV value of right caudate from slope of Logan plot using blood input function (top) and estimate of B_{max}/K_d + 1 of right caudate from slope of Logan plot using occipital cortical input function (bottom).

Table 3 shows the results of linear regression analysis between the different measures. For the first scan, there was no significant correlation between total DV values and any of the other measures ($P > 0.05$). For the second scan, the total DV values correlated with some of the other measures, but not at all with others (e.g., DV_{CAU} correlates with CAU/OC but not with $B_{max}/K_{d(CAU/OC)}$). For both first and second scans, there were significant correlations between radioactivity ratio, plasma-input B_{max}/K_d and tissue-input B_{max}/K_d ($P < 0.05$).

DISCUSSION

In this study, the reproducibility of different measures of DTBZ binding was assessed using both the reliability and the absolute percent change as metrics. The absolute change between two scans is commonly used to assess reproducibility and allows one to simply determine the change in the values of the measure between the first and the second scans. With the exception of plasma-input total DV, the absolute percent change in any of the other measures was below 15% for any subject (average 4%–7%), indicating reasonable reproducibility. R, on the other hand, is a statistical measure for reproducibility that is more powerful than the absolute percent change (*18*) and takes into consideration the SDB and SDW. Thus, those measures with an SDW as large as the SDB would result in a lower reliability, despite a low absolute percent change. The total DV measures gave the lowest reliability of all the measures (with the highest average percent change). Whereas the reproducibility of all measures is subject to variation from subject positioning, biological variability and PET measurement, total DV values are subject to an additional source of variability arising from the use of a metabolite-corrected plasma activity curve. Thus, the low reliability of the plasma-input total DV values likely reflects the additional variability introduced by blood sampling and metabolite analysis.

The tracer used in this study was a racemic mixture of the (+) and (–) enantiomers. The analysis methods used are all based on equilibrium measures and remain valid even though the two compounds have distinct kinetic behaviors. However, because only the (+) enantiomer binds specifically to the vesicular transporter, the binding potential values determined in this study would be expected to be about half those obtained with the active enantiomer alone.

DTBZ binds to VMAT and is therefore not specific to

TABLE 1
Results of One-Way Analysis of Variance on Different Measures for DTBZ (n = 10) Using Occipital Cortex or Cerebellum Reference Region

	Mean	SDB (CV)	SDW (CV)	95% CI	R
Radioactivity ratios					
CAU/OC	1.90	0.10 (5.3)	0.10 (5.4)	0.07–0.18	49%
PUT/OC	1.80	0.18 (9.8)	0.10 (5.4)	0.07–0.17	77%
CAU/CE	1.76	0.40 (6.6)	0.32 (5.3)	0.22–0.55	61%
PUT/CE	1.67	0.53 (9.4)	0.33 (5.8)	0.23–0.58	72%
Logan plasma-input DV and B_{max}/K_d					
DV_{CAU}	10.42	0.65 (6.2)	1.14 (10.9)	0.79–2.00	24%
DV_{PUT}	9.88	0.84 (8.5)	1.07 (10.8)	0.75–1.88	38%
DV_{OC}	5.76	0.29 (5.0)	0.63 (11.0)	0.44–1.11	17%
DV_{CE}	6.68	0.58 (8.7)	0.67 (10.1)	0.47–1.18	43%
$B_{max}/K_{d(CAU/OC)}$	0.81	0.09 (5.1)	0.06 (3.5)	0.04–0.11	68%
$B_{max}/K_{d(PUT/OC)}$	0.72	0.16 (9.2)	0.07 (4.2)	0.05–0.13	82%
$B_{max}/K_{d(CAU/CE)}$	0.57	0.07 (4.5)	0.08 (5.4)	0.06–0.15	41%
$B_{max}/K_{d(PUT/CE)}$	0.49	0.11 (7.7)	0.08 (5.4)	0.06–0.14	67%
Logan tissue-input B_{max}/K_d					
$B_{max}/K_{d(CAU/OC)}$	0.78	0.09 (4.8)	0.06 (3.4)	0.04–0.11	67%
$B_{max}/K_{d(PUT/OC)}$	0.69	0.15 (8.8)	0.07 (4.0)	0.05–0.12	83%
$B_{max}/K_{d(CAU/CE)}$	0.54	0.08 (4.9)	0.07 (4.8)	0.05–0.13	51%
$B_{max}/K_{d(PUT/CE)}$	0.46	0.11 (7.6)	0.07 (4.8)	0.05–0.12	71%

DTBZ = dihydrotetrabenazine; SDB = standard deviation between subjects; SDW = standard deviation within subjects; CV = coefficient variation; 95% CI = 95% confidence interval of SDW; R = reliability; CAU = caudate; OC = occipital cortex; PUT = putamen; CE = cerebellum; DV = distribution volume; B_{max}/K_d = binding potential.

TABLE 2
Absolute Percent Change in Values of Measures Between First and Second Scan

	Absolute % change*	
	Mean ± 1 SD	Range
Radioactivity ratios		
CAU/OC	3.9 ± 4.0	0.26–9.89
PUT/OC	5.0 ± 3.8	1.07–13.87
CAU/CE	5.7 ± 4.0	0.58–11.78
PUT/CE	6.5 ± 4.1	0.42–14.77
Logan plasma-input DV and B_{max}/K_d +1		
DV_{CAU}	11.6 ± 14.6	1.80–40.30
DV_{PUT}	11.6 ± 13.9	0.20–38.25
DV_{OC}	11.4 ± 13.7	1.28–35.56
DV_{CE}	11.9 ± 12.4	1.48–33.03
$B_{max}/K_{d(CAU/OC)}$ +1	3.5 ± 3.6	0.02–8.79
$B_{max}/K_{d(PUT/OC)}$ +1	5.1 ± 3.0	1.99–11.10
$B_{max}/K_{d(CAU/CE)}$ +1	6.6 ± 3.9	1.64–10.81
$B_{max}/K_{d(PUT/CE)}$ +1	6.9 ± 3.4	1.26–10.77
Logan tissue-input B_{max}/K_d+1		
$B_{max}/K_{d(CAU/OC)}$ +1	3.6 ± 3.3	0.51–8.55
$B_{max}/K_{d(PUT/OC)}$ +1	4.7 ± 2.9	1.37–9.81
$B_{max}/K_{d(CAU/CE)}$ +1	5.9 ± 3.6	1.39–13.17
$B_{max}/K_{d(PUT/CE)}$ +1	6.3 ± 2.8	0.91–9.58

*Absolute percent change calculated as [(value of second scan − value of first scan)/mean of the values of the two scans] × 100%.

CAU = caudate; OC = occipital cortex; PUT = putamen; CE = cerebellum; DV = distribution volume; B_{max}/K_d = binding potential.

dopaminergic nerve terminals. However, because the majority (>95%) of monoaminergic terminals in the striatum are dopaminergic terminals (*19*), the PET signal measured with (±)-α-[^{11}C]DTBZ in the striatum is largely a reflection of dopaminergic nerve terminal density.

Because no brain region is completely devoid of VMAT, none can truly be regarded as a "reference." However, the cerebellum and occipital cortex are monoamine-poor areas and are frequently used as reference regions for evaluating striatal dopamine uptake or dopamine receptor binding with a variety of other tracers. We therefore examined the reliability of using cerebellum or occipital cortex as potential reference regions for the bloodless analysis of DTBZ PET data. Several studies with other tracers have demonstrated that reliability improved substantially when the ratio of the DV, i.e., $DV_{target}/DV_{reference}$ (presented as plasma-input B_{max}/K_d) as opposed to the DVs alone was used (*20,21*). This study confirmed this. The reliability of both plasma and tissue-input B_{max}/K_d was significantly better than that of total DV values.

Measures using the occipital cortex as the reference region had higher reliability than the same measures using the cerebellum as the reference region. Values using the occipital cortex as the reference region were also consistently higher. Thus, although the measures using either cerebellum or occipital cortex as the reference region consistently correlated with each other (Table 3), the occipital cortex would seem to be a better choice as the reference region. However, because neither the occipital cortex nor the cerebellum is devoid of monoaminergic inputs (norepineph-

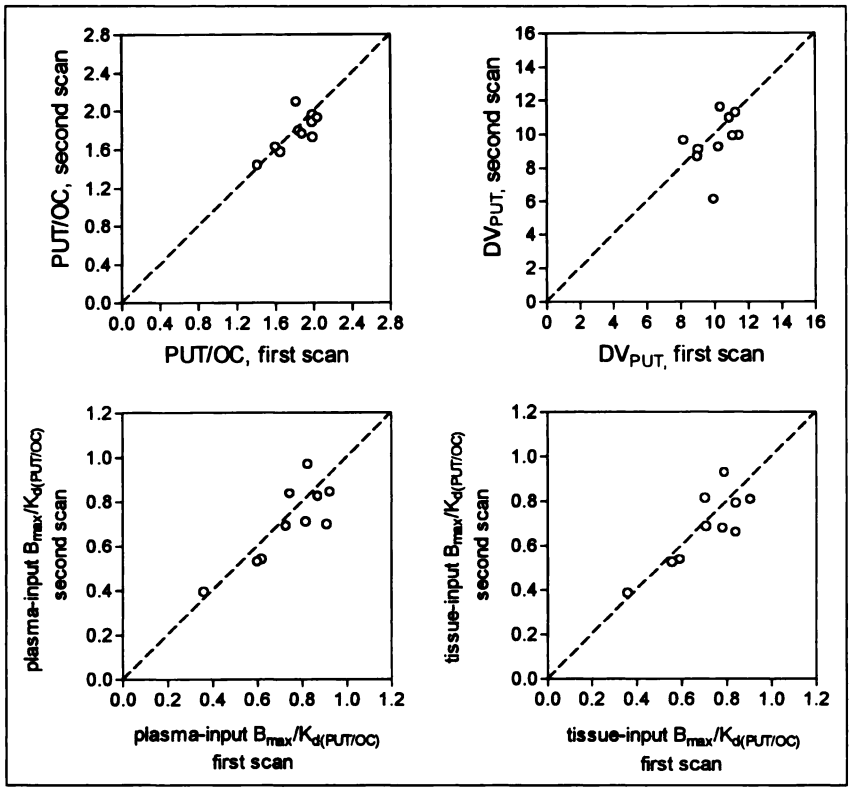

FIGURE 4. Reproducibility of several extracted measures, presented as values derived from second scan plotted against those from first scan. Data for putamen are presented as representative. Derived measures include radioactivity ratios, plasma-input total DV, plasma-input B_{max}/K_d and tissue-input B_{max}/K_d. Dashed lines represent perfect-agreement lines between values of first and second scans.

TABLE 3
Linear Correlation Analysis Between Different Measures for DTBZ Using Occipital Cortex or Cerebellum as Reference Region

	First Scan		Second Scan	
	r	P	r	P
Occipital cortex as reference region				
CAU/OC versus DV_{CAU}	0.256	0.476	0.653	0.041*
CAU/OC versus plasma-input $B_{max}/K_{d(CAU/OC)}$	0.954	<0.0001*	0.975	<0.0001*
CAU/OC versus tissue-input $B_{max}/K_{d(CAU/OC)}$	0.956	<0.0001*	0.969	<0.0001*
DV_{CAU} versus tissue-input $B_{max}/K_{d(CAU/OC)}$	0.143	0.693	0.580	0.079
plasma-input $B_{max}/K_{d(CAU/OC)}$ versus tissue-input $B_{max}/K_{d(CAU/OC)}$	0.981	<0.0001*	0.992	<0.0001*
PUT/OC versus DV_{PUT}	0.397	0.256	0.748	0.013*
PUT/OC versus plasma-input $B_{max}/K_{d(PUT/OC)}$	0.973	<0.0001*	0.988	<0.0001*
PUT/OC versus tissue-input $B_{max}/K_{d(PUT/OC)}$	0.976	<0.0001*	0.993	<0.0001*
DV_{PUT} versus tissue-input $B_{max}/K_{d(PUT/OC)}$	0.347	0.326	0.700	0.024*
plasma-input $B_{max}/K_{d(PUT/OC)}$ versus tissue-input $B_{max}/K_{d(PUT/OC)}$	0.996	<0.0001*	0.999	<0.0001*
Cerebellum as reference region				
CAU/CE versus DV_{CAU}	0.267	0.456	0.439	0.204
CAU/CE versus plasma-input $B_{max}/K_{d(CAU/CE)}$	0.862	0.001*	0.946	<0.001*
CAU/CE versus tissue-input $B_{max}/K_{d(CAU/CE)}$	0.883	0.001*	0.937	<0.001*
DV_{CAU} versus tissue-input $B_{max}/K_{d(CAU/CE)}$	0.187	0.605	0.182	0.615
plasma-input $B_{max}/K_{d(CAU/CE)}$ versus tissue-input $B_{max}/K_{d(CAU/CE)}$	0.989	<0.0001*	0.994	<0.0001*
PUT/CE versus DV_{PUT}	0.320	0.367	0.647	0.043*
PUT/CE versus plasma-input $B_{max}/K_{d(PUT/CE)}$	0.913	0.0002*	0.964	<0.0001*
PUT/CE versus tissue-input $B_{max}/K_{d(PUT/CE)}$	0.927	0.0001*	0.972	<0.0001*
DV_{PUT} versus tissue-input $B_{max}/K_{d(PUT/CE)}$	0.273	0.446	0.491	0.150
plasma-input $B_{max}/K_{d(PUT/CE)}$ versus tissue-input $B_{max}/K_{d(PUT/CE)}$	0.992	<0.0001*	0.997	<0.0001*

*$P < 0.05$, slope significantly different from zero.

DTBZ = dihydrotetrabenazine; CAU = caudate; OC = occipital cortex; DV = distribution volume; B_{max}/K_d = binding potential; PUT = putamen; CE = cerebellum.

rine for example), the use of a reference region, whether the occipital cortex or the cerebellum, should be considered with caution and decided on a study-by-study basis. Although the use of a "bloodless" scanning protocol is an attractive alternative, because it reduces the burden on both the subjects (arterial line) and the PET scientists (blood sampling and metabolite analysis), it may be inappropriate when studying patients with possible or suspected abnormalities of the reference regions themselves (either anatomic or metabolic) or abnormalities of the monoaminergic system innervating them. Thus, preliminary studies using a plasma input function are necessary to ascertain the feasibility of using the cerebellum or occipital cortex as the input function in an individual patient.

In the original derivation of the tissue-input distribution volume ratio method (*16*), the reference tissue is assumed to be free of specific binding. Fits of the reference tissue time courses with a one-tissue-compartment model are performed to provide the population mean values of the kinetic rate constants required for the analysis. However, because of the small but significant specific binding of DTBZ in both the cerebellum and occipital cortex, these compartmental fits did not reproduce the data exactly, and the resulting distribution volume ratios must be considered to be approximate. The ratios derived by the tissue-input approach were consistently slightly smaller than those derived by the plasma-input approach (Tables 1 and 3). The implementation of the tissue-input method with specific binding in the reference tissue taken fully into account is part of a thorough investigation of the method currently underway in our laboratory.

Frey et al. (*12*) have reported a significant age-related decline in VMAT density measured with [^{11}C]DTBZ. We examined the effect of aging on VMAT density using the data from the first scans of our subjects. Although there seemed to be a trend toward age-related decline, no significant correlation was found between subject age and any of the measures. Further studies in a larger population are warranted.

CONCLUSION

(±)-α-[^{11}C]DTBZ is a reliable PET tracer that provides reproducible in vivo measurement of striatal VMAT density. Both the occipital cortex and cerebellum appear to be appropriate "reference" regions for DTBZ PET data analysis, with the occipital cortex exhibiting a higher reliability than cerebellum. Radioactivity ratios (target-to-reference), plasma-input B_{max}/K_d and tissue-input B_{max}/K_d all have higher reliability than plasma-input total DV values. However, if a reference region is used, caution must be exercised in circumstances when DTBZ binding in these reference regions may be altered.

ACKNOWLEDGMENTS

This study was supported by the Medical Research Council of Canada. We thank Hoffman La Roche for supplying tetrabenazine from which the precursor was made. The authors would also like to acknowledge the contributions to this work by Barbara Legg, Carolyn English, Edwin Mak, Dr. Jain Ming Lu, Jess Wudel, Joe M. Huser, Salma Jivan and the TRIUMF PET group.

REFERENCES

1. Pletscher A, Brossi A, Grey KF. Benzoquinoline derivatives: a new class of monoamine decreasing drugs with psychotropic action. *Int Rev Neurobiol.* 1962;4:275–306.
2. Henry JP, Scherman D. Radioligands of the vesicular monoamine transporter and their use as markers of monoamine storage vesicles. *Biochemical Pharmacol.* 1989;38:2395–2404.
3. Vander Borght TM, Kilbourn MR, Koeppe RA, et al. In vivo imaging of the brain vesicular monoamine transporter. *J Nucl Med.* 1995;36:2252–2260.
4. Masuo Y, Pelaprat D, Scherman D, Rostene W. 3-H-dihydrotetrabenazine, a new marker for the visualization of dopaminergic denervation in the rat striatum. *Neurosci lett.* 1990;114:45–50.
5. Near JA. [^{3}H]Dihydrotetrabenazine binding to bovine striatal synaptic vesicles. *Mol Pharmacol.* 1986;30:252–257.
6. Lehericy S, Brandel JP, Hirsch EC, et al. Monoamine vesicular uptake sites in patients with Parkinson's disease and Alzheimer's disease, as measured by tritiated dihydrotetrabenazine autoradiography. *Brain Res.* 1994;659:1–9.
7. Thibaut F, Faucheux BA, Marquez J, et al. Regional distribution of monoamine vesicular uptake sites in the mesencephalon of control subjects and patients with Parkinson's disease: a postmortem study using tritiated tetrabenazine. *Brain Res.* 1995;692:233–243.
8. Vander Borght T, Kilbourn M, Desmond T, Kuhl D, Frey K. The vesicular monoamine transporter is not regulated by dopaminergic drug treatments. *Eur J Pharmacol.* 1995;294:577–583.
9. Wilson JM, Kish SJ. The vesicular monoamine transporter, in contrast to the dopamine transporter, is not altered by chronic cocaine self-administration in the rat. *J Neurosci.* 1996;16:3507–3510.
10. Koeppe RA, Frey KA, Vander Borght TM, et al. Kinetic evaluation of [^{11}C]dihydrotetrabenazine by dynamic PET: measurement of vesicular monoamine transporter. *J Cereb Blood Flow Metab.* 1996;16:1288–1299.
11. Koeppe RA, Frey KA, Vander Borght TM, et al. Kinetic evaluation of alpha-[C-11]dihydrotetrabenazine (DTBZ): a PET ligand for assessing the vesicular monoamine transporter [abstract]. *J Nucl Med.* 1995;36:118P.
12. Frey KA, Koeppe RA, Kilbourn MR, et al. Presynaptic monoaminergic vesicles in Parkinson's disease and normal aging. *Ann Neurol.* 1996;40:873–884.
13. Gilman S, Frey KA, Koeppe RA, et al. Decreased striatal monoaminergic terminals in olivopontocerebellar atrophy and multiple system atrophy demonstrated with positron emission tomography. *Ann Neurol.* 1996;40:885–892.
14. Kilbourn MR, Lee LC, Vander Borght TM, Jewett DM, Frey KA. Binding of alpha-dihydrotetrabenazine to the vesicular monoamine transporter is stereospecific. *Eur J Pharmacol.* 1995;278:249–252.
15. Logan J, Fowler JS, Volkow ND, et al. Graphical analysis of reversible radioligand binding from time-activity measurements applied to [N-^{11}C-methyl]-(-)-cocaine PET studies in human subjects. *J Cereb Blood Flow Metab.* 1990;10:740–747.
16. Logan J, Fowler JS, Volkow ND, Wang GJ, Ding YS, Alexoff DL. Distribution volume ratios without blood sampling from graphical analysis of PET data. *J Cereb Blood Flow Metab.* 1996;16:834–840.
17. Scheffe H. *The Analysis of Variance.* New York, NY: Wiley & Sons; 1959:221–260.
18. Fleiss JL. *The Design and Analysis of Clinical Experiments.* New York, NY: Wiley & Sons; 1986.
19. Kish SJ, Robaitaille Y, El-Awar M, et al. Striatal monoamine neurotransmitters and metabolites in dominantly inherited olivopontocerebellar atropy. *Neurology.* 1992;42:1573–1577.
20. Logan J, Volkow ND, Fowler JS, et al. Effects of blood flow on [11-C]raclopride binding in the brain: model simulations and kinetic analysis of PET data. *J Cereb Blood Flow Metab.* 1995;14:995–1010.
21. Chan GLY, Holden JE, Stoessl AJ, Doudet DJ, Wang Y, Dobko T. Reproducibility of the distribution of carbon-11-SCH 23390, a dopamine D_1 receptor tracer, in normal subjects. *J Nucl Med.* 1998;39:792–797.